

Modeling space plasma dynamics with anisotropic Kappa distributions

M. Lazar, V. Pierrard, S. Poedts and R. Schlickeiser

Abstract Space plasmas are collisionpoor and kinetic effects prevail leading to wave fluctuations, which transfer the energy to small scales: wave-particle interactions replace collisions and enhance dispersive effects heating particles and producing suprathermal populations observed at any heliospheric distance in the solar wind. At large distances collisions are not efficient, and the selfgenerated instabilities constrain the solar wind anisotropy including the thermal core and the suprathermal components. The generalized power-laws of Kappa-type are the best fitting model for the observed distributions of particles, and a convenient mathematical tool for modeling their dynamics. But the anisotropic Kappa models are not correlated with the observations leading, in general, to inconsistent effects. This review work aims to reconcile some of the existing Kappa models with the observations.

1 Introduction

Direct *in-situ* measurements in the solar wind and terrestrial magnetosphere indicate that the velocity distribution functions (VDF) of space plasma particles are

M. Lazar

Institut für Theoretische Physik, Lehrstuhl IV: Weltraum- und Astrophysik, Ruhr-Universität Bochum, D-44780 Bochum, Germany, e-mail: mlazar@tp4.rub.de

V. Pierrard

Belgian Institute for Space Aeronomy, Space Physics, av. circulaire 3, 1180 Brussels, Belgium e-mail: viviane.pierrard@oma.be

S. Poedts

Centre for Plasma Astrophysics, Celestijnenlaan 200B, 3001 Leuven, Belgium, e-mail: Stefaan.Poedts@wis.kuleuven.be

R. Schlickeiser

Institut für Theoretische Physik, Lehrstuhl IV: Weltraum- und Astrophysik, Ruhr-Universität Bochum, D-44780 Bochum, Germany, e-mail: rsch@tp4.rub.de

quasi-Maxwellian up to the mean thermal velocities (the core component), while they exhibit non-Maxwellian suprathermal tails (the halo component) at higher energies (see recent reviews of Marsch (2006)[1] and Pierrard & Lazar (2010)[2], and references therein). Processes by which the suprathermal particles are produced and accelerated [3, 4, 5, 6, 7, 8] are of increasing interest for applications in astrophysics and laboratory or fusion plasma devices where they are known as the *runaway* particles decoupled from the thermal state of motion. The solar wind generally appears to involve an abundance of suprathermal electrons and ions observed to occur in the interplanetary medium, and their analysis provides valuable information about their source, whether it is in the Sun or outer heliosphere.

Accelerated particles (including electrons, protons and minor ions) are detected at any heliospheric distance in the quiet wind as well as in the solar energetic particle (SEP) events associated to flares and coronal mass ejections (CMEs) during solar maximum (see reviews by Lin (1998)[9] and Pierrard & Lazar (2010)[2]). A steady-state suprathermal ion population is observed throughout the inner heliosphere with a VDF close to $\sim v^{-5}$ [10], and, on the largest scales, the relativistic cosmic-ray gas also plays such a dynamical role through the galaxy and its halo [11].

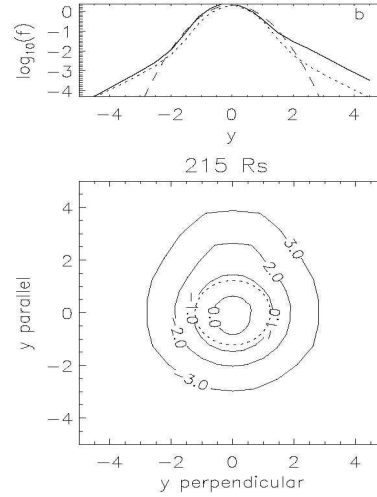
2 Wave instability constraints of the suprathermal anisotropy

Nonthermal features and kinetic anisotropies like temperature anisotropies, heat fluxes or particle streams are also a characteristic of the solar wind and near the Earth's magnetosphere [1]. At low altitudes in the solar wind, velocity distributions of plasma particles regularly show an excess of kinetic energy transverse to the local mean magnetic field ($T_{\perp} > T_{\parallel}$, where \perp , and \parallel denote directions with respect to the magnetic field) most probably due to the compression exerted by the strong guiding magnetic field near the Sun. At larger heliospheric distances, the anisotropy is controlled by the Chew-Goldberger-Low mechanism: the adiabatic expansion of the poorcollision plasma increases the pressure and temperature along the magnetic field leading to $T_{\parallel} > T_{\perp}$. In more violent interplanetary shocks resulting after solar flares and coronal mass ejections (CME), injection of particle beams into the ionized interplanetary medium creates additional anisotropy [1, 9].

The high rate of occurrence of an excess of perpendicular temperature ($T_{\perp} > T_{\parallel}$) in measurements at large distances [13, 14] is a proof that other mechanisms of acceleration, namely, the wave-particle interaction, must be at work there dominating the adiabatic expansion. Indeed, large deviations from isotropy quickly relax by the resulting wave instabilities, which act either to scatter particles back to isotropy, or to accelerate lower energetic particles (Landau or cyclotron heating) and maintain a suprathermal abundance because thermalization is not efficient at these scales [1].

None of these processes is well understood, mostly because these plasmas are low-collisional and require progress in modeling the wave turbulence, going beyond MHD models to use a kinetic and selfconsistent description. In such plasmas transport of matter and energy is governed by the selfcorrelation between particles and

Fig. 1 Electron velocity distributions observed by *Wind* mission at 1 AU, as energy spectra (top) parallel (solid) and perpendicular (dashed) to magnetic field; and velocity space contours (bottom) in a high-speed solar wind. Note the anisotropic isodensity contours, less for the core and more pronounced for the halo and the strahl in fast solar wind (after Pierrard et al. (1999) [12]).



electromagnetic fields, which can, for instance, convect charged particles in phase space but are themselves created by these particles. Thus, the suprathermal populations involve selfconsistently in both processes of wave turbulence generation and particle energization, and the resulting Kappa functions that elegantly describes distributions measured in the solar wind [2], represent therefore not only a convenient mathematical tool, but a natural and quite general state of the plasma [15].

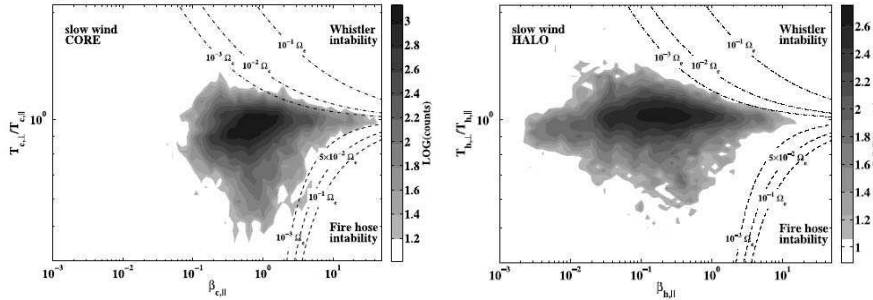


Fig. 2 Solar wind electron temperature anisotropy (T_{\perp}/T_{\parallel}) versus β_{\parallel} : the instability thresholds from a bi-Maxwellian model do not constrain the suprathermal halo (after Stverak et al. (2008)).

While the thermal core in the solar wind is less anisotropic, the superthermal halo has in general a pronounced temperature anisotropy ($T_{\perp} \neq T_{\parallel}$) with respect to the local magnetic field [1, 2]. Deformations of the VDFs observed in the solar wind are not as strong as one would expect from a free motion of particles (Kasper et al. 2002, Stverak et al. 2008, Bale et al. 2009). Because collisions are not effective, any increase of kinetic anisotropy is limited by converting the excess of free energy into electromagnetic fluctuations, and pitch-angle diffusion. Model-

ing the VDF with a bi-Maxwellian, the instability thresholds shape precisely the core (Fig. 2, left) but show regularly an important departure from to the halo limits (Fig. 2, right). While the whistler instability limits the perpendicular temperature to grow ($T_{\perp} > T_{\parallel}$), the firehose instability constrains any excess of parallel temperature ($T_{\perp} < T_{\parallel}$). Suprathermal particles cannot fit into a Maxwellian approach ($\kappa \rightarrow \infty$), but must be modeled with an appropriate Kappa function. A bi-Kappa (or bi-Lorentzian) function has extensively been used to model gyrotropic distributions and their dispersion/stability properties [16, 17]

$$F_1(v_{\parallel}, v_{\perp}) = \frac{1}{\pi^{3/2} w_{\perp}^2 w_{\parallel}} \frac{\Gamma[\kappa+1]}{\kappa^{3/2} \Gamma[\kappa-1/2]} \left(1 + \frac{v_{\parallel}^2}{\kappa w_{\parallel}^2} + \frac{v_{\perp}^2}{\kappa w_{\perp}^2} \right)^{-\kappa-1}. \quad (1)$$

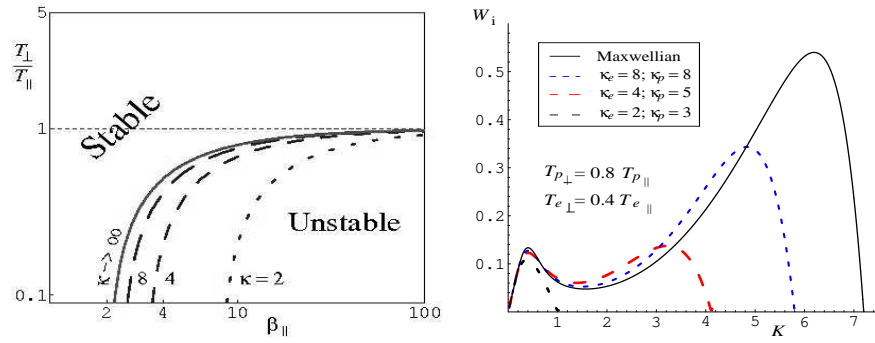


Fig. 3 Firehose instability: thresholds (left) and growth rates (right) from a bi-Kappa model.

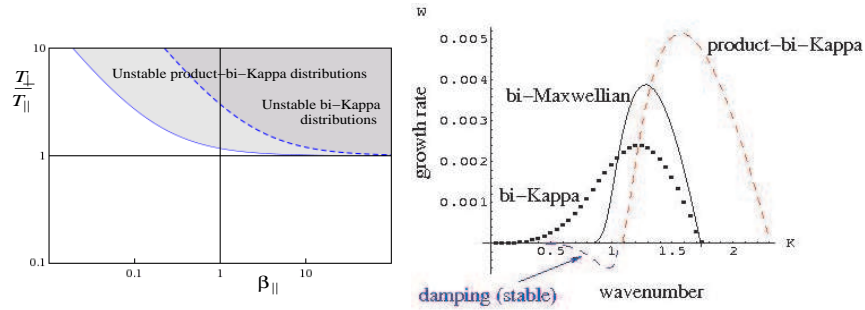


Fig. 4 Whistler instability: thresholds (left) and growth rates (right) from three different models: the bi-Kappa, the product-bi-Kappa and the bi-Maxwellian (after Lazar et al. (2011a)).

However, this model does not provide the expected better fits to the observations. For instance, both instabilities of interest for the electron populations, the whistler

and the firehose, are inhibited and threshold constraints do not approach but rather depart from the measured limits of the halo [18, 19, 21, 22]. Marginal conditions of the firehose instability are illustrated in Fig. 3 (left) showing the need for a larger temperature anisotropy and a larger plasma $\beta_{\parallel} \equiv 8\pi nk_B T_{\parallel}/B_0^2$ to produce the instability in Kappa distributed plasmas (low values of $\kappa \rightarrow 3/2$). By comparison to a bi-Maxwellian ($\kappa \rightarrow \infty$), the growth rates are in general reduced and restrained to small wavenumbers (Fig. 3, right) [19, 22]. The same tendency is observed in the evolution of the whistler instability (Fig. 4): by comparison to a bi-Maxwellian thresholds do not depart much, but the growth rates decrease significantly for lower values of the index κ (Fig. 4, right) [18, 21].

3 Product-bi-Kappa model

It is evident that a novel Kappa function is needed to model kinetic anisotropies and to incorporate the excess of free energy expected to exist in suprathermal anisotropic plasmas providing better fit to the observations. Recently a new approach has been proposed [20, 21, 23] based on the anisotropic product-bi-Kappa function [16]

$$F_2(v_{\parallel}, v_{\perp}) = \frac{w_{\perp}^{-2}}{\pi^{3/2} w_{\parallel}} \frac{\Gamma[\kappa_{\parallel} + 1]}{\kappa_{\parallel}^{1/2} \Gamma[\kappa_{\parallel} + 1/2]} \left(1 + \frac{v_{\parallel}^2}{\kappa_{\parallel} w_{\parallel}^2}\right)^{-\kappa_{\parallel}-1} \left(1 + \frac{v_{\perp}^2}{\kappa_{\perp} w_{\perp}^2}\right)^{-\kappa_{\perp}-1}. \quad (2)$$

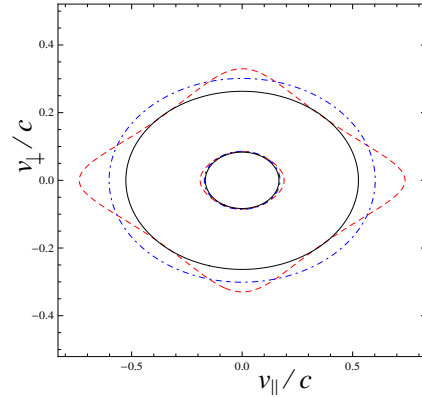
By contrast to the bi-Kappa function (1), which seems to be less realistic because the two degrees of freedom are coupled and controlled by the same power index κ , the new product-bi-Kappa function shows an advanced flexibility in modeling gyrotropic VDFs with two distinct temperatures $T_{\parallel, \perp}$ and two distinct power indices $\kappa_{\parallel, \perp}$. Thus, a new concept for the particle anisotropy can be introduced by including both anisotropies of the temperatures $T_{\parallel} \neq T_{\perp}$ and the Kappa indices $\kappa_{\parallel} \neq \kappa_{\perp}$. The analysis becomes therefore more relevant but complicated and this is probably the reason this model was only occasionally invoked (after Summers & Thorne (1991) proposed it), merely in a simplified Maxwellian-Kappa form [17]

$$F_3(v_{\parallel}, v_{\perp}) = \frac{w_{\perp}^{-2}}{\pi^{3/2} w_{\parallel}} \frac{\Gamma[\kappa + 1]}{\kappa^{1/2} \Gamma[\kappa + 1/2]} \left(1 + \frac{v_{\parallel}^2}{\kappa w_{\parallel}^2}\right)^{-\kappa-1} \exp\left(-\frac{v_{\perp}^2}{w_{\perp}^2}\right). \quad (3)$$

The distribution function (2) reduces to distribution function (3) in the limit of very large values of $\kappa_{\perp} \rightarrow \infty$. Thus both forms of the new model represented by the general distribution function (2) or by the particular form (3) reduce to the same bi-Maxwellian in the limit of very large power indices ($\kappa_{\parallel, \perp} \rightarrow \infty$).

Contour plots in velocity plane are illustrated in Fig. 5 showing no visible excess of asymmetry of the bi-Kappa (dotted-dashed lines) by comparison to the bi-Maxwellian (solid lines), but a prominent asymmetry and anisotropy of the new product-bi-Kappa distribution function (dashed lines) by comparison to both the bi-

Fig. 5 Two sets of contours, one close to maximum and one close to the minimum base: the bi-Maxwellians ($\kappa_{\parallel} = \kappa_{\perp} \rightarrow \infty$) with solid lines, product-bi-Kappas with red dashed lines, and bi-Kappas with blue dotted-dashed lines (for the same $v_{T,\parallel}/c = 2v_{T,\perp}/c = 0.2$, and $\kappa_{\parallel} = \kappa_{\perp} = 3$).



Maxwellian and bi-Kappa distribution functions, even for the same temperatures $T_{\parallel} = T_{\perp}$, and the same $\kappa_{\parallel} = \kappa_{\perp} = \kappa$ [20, 21]. However, the new distribution model and its dispersion properties and stability must directly be confronted to the observations in the solar wind and terrestrial magnetosphere.

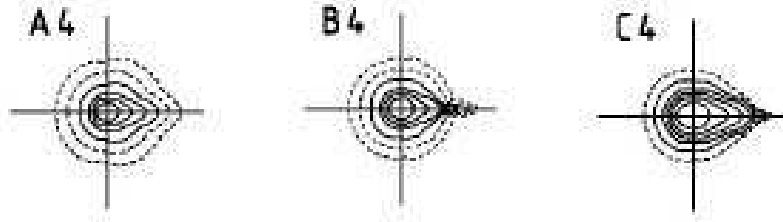


Fig. 6 The electron VDF with a strahl component in the high speed solar wind at a distance (in AU) $R = 0.98$ (left), $0.64 \leq R \leq 0.70$ (middle) and $0.29 \leq R \leq 0.34$ (right) (after Pilipp et al. 1987a).

Thus, contours of the electron distribution functions measured at different heliospheric distances in a high speed solar wind (see Figs. 6 and 7) show such skewed, highly anisotropic tails along the magnetic field direction [27, 28], which look quite similar to the product-bi-Kappa contours in Fig. 5. In Fig. 6, skews of the electron distributions are asymmetric being produced by the magnetic field aligned strahl population, which is highly energetic (suprathermal) and antisunward moving [27]. The presumable origin of the strahl electrons is in the energetic ejecta from the coronal holes, and radial evolution show a decreasing with distance from the Sun in the favor of the halo population, which is enhancing [29]. The strahl component is the main driver of the (electron) heat flux, and the main contributor to the anisotropy of suprathermals, apparently a manifestation of the adiabatic focusing.

The quite-time distribution in the fast solar wind (Fig. 6) is modeled by the product-bi-Kappa function only on one side, namely, the outward direction ($v_{\parallel} > 0$), while semicontours in the backward direction are similar to a bi-Kappa (low anisotropic) model. Analytically one can combine the Eqs. (2) and (3) to form

$$F_4(v_{\parallel}, v_{\perp}) = H[-v_{\parallel}] C_L \left(1 + \frac{v_{\parallel}^2}{\kappa_L w_{L,\parallel}^2} + \frac{v_{\perp}^2}{\kappa_L w_{L,\perp}^2} \right)^{-\kappa_L - 1} + H[v_{\parallel}] C_R \left(1 + \frac{v_{\parallel}^2}{\kappa_R w_{R,\parallel}^2} \right)^{-\kappa_R - 1} \exp\left(-\frac{v_{\perp}^2}{w_{R,\perp}^2}\right), \quad (4)$$

where $H[x]$ is the Heaviside function, and $C_{L,R}$ are normalization constants. Contour plots are similar to the one-sided strahl observations in Fig. 6. Hence the immediate effect would be a corresponding asymmetric spectrum of the selfgenerated wave fluctuations, which are expected to dominate the outward direction. The future work should explore the stability of this new model and correlate with the observations.

Electron distribution functions (see Fig. 7) with an unusual double strahl have been observed on rare occasions in the solar wind by Helios probes [28]. Contour plots of these distribution function are illustrated in Fig. 7 (left) and show a strong symmetric bidirectional anisotropy very similar to the product-bi-Kappa model in Fig. 5. Double-strahl distributions would be observed if the spacecraft was fortuitously near the outer end of a magnetic loop connected to the Sun, and electrons coming from both foot points have traveled roughly the same distance and thus may form a symmetric distribution with a counterstreaming strahl aspect. A similar distribution is expected in the observations if the spacecraft was at the outer end of a disconnected large scale loop [28].

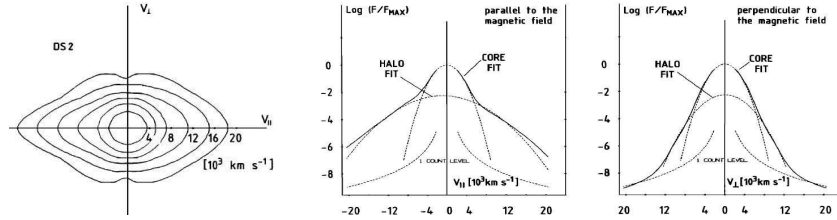


Fig. 7 Contours and one-dimensional cuts of unusual double-strahl distribution function observed by Helios (after Pilipp et al. 1987b).

Another important confirmation should come from the resulting electromagnetic fluctuations which constrain particle velocity anisotropy to grow [14, 24]. Some preliminary analysis have indeed shown that the whistler instability growth rates (see Fig. 4, right) calculated for the general product-bi-Kappa model are enhanced (dashed line) by comparison to those obtained for a bi-Maxwellian (solid line) or a bi-Kappa model (dotted line), and the instability thresholds illustrated in Fig. 4 (left) tend to approach better the limits of the electron halo in Fig. 2 (right) [21]. Unlike

the bi-Maxwellian or bi-Kappa distributions, the product-bi-Kappa anisotropy can be stable against the excitation of the low-wavenumber whistler waves, the critical wavenumber $k_c \simeq \Omega / (\theta_{\parallel} \sqrt{\kappa_{\parallel} A})$ is vanishing only for $\kappa_{\parallel} \rightarrow \infty$ (Maxwellian plasma). Moreover, it was shown the instability of an asymmetric Maxwellian-Kappa distribution without an effective temperature anisotropy ($T_{\perp} = T_{\parallel}$) against the excitation of the whistler waves propagating obliquely to the magnetic field [30], most probably due to the same asymmetry of contours in velocity space (Fig. 5). Thus, the new product-bi-Kappa model seems to incorporate the excess of free energy expected to exist in anisotropic suprathermal plasmas. For the opposite case ($T_{\parallel} > T_{\perp}$), the fire-hose instability is currently under active investigations, and, according to the preceding discussion, we expect that a product-bi-Kappa model will enhance the growth rates and provide better agreement of the marginal stability with the observed limits of the halo (Fig. 2, right).

Generation of such asymmetric distribution profiles is also supported by the anisotropic turbulence of the solar wind, where the acceleration is expected to occur either perpendicular (cyclotron damping)[5] or in direction (Landau damping)[6] of the interplanetary magnetic field. The nonlinear wave-wave and wave-particle couplings involving intense low-frequency Alfvén waves or electrostatic Langmuir and ion sound (weak) turbulence driven by the beam-plasma instabilities can also be responsible for the acceleration in the corona, solar wind and magnetosphere [4, 7]. However, these models do not provide much guidance on a full 3D evolution of the distribution function and its nonthermal features, like suprathermal tails and kinetic anisotropies, in the acceleration process. This task is still complicated, but will, hopefully, make the object of the next investigations.

4 Conclusions and perspectives

A large variety of nonthermal features like temperature anisotropies, heat fluxes or particle streams are permanently observed in the solar wind and near the Earth's magnetosphere [1, 2]. These do not grow indefinitely, but tend to regulate themselves since they contain sufficient free energy to drive plasma instabilities and micro-turbulence [25]. Plasma wave turbulence provides the main dissipation mechanisms maintaining a fluid-like behavior of the plasma in spite of the fact that collisional free paths become comparable to the large scales of the heliosphere. Bi-Maxwellian models have extensively been used to describe particle distributions and their dynamics in the solar wind, but the observations clearly indicate the relevance of Kappa distribution functions which incorporate both the quasithermal core and the suprathermal halo. Because the anisotropic Kappa functions are not correlated, in general, with the observations, here we have reviewed these models, and established their direct or indirect confirmations by the observations.

The nondrifting distribution functions used to describe the temperature anisotropy of the different plasma components (with respect to the magnetic field), are the bi-Kappa and product-bi-Kappa functions. The bi-Kappa function seems less realistic

because the two degrees of freedom parallel and perpendicular to the magnetic field are coupled and controlled by the same power index k . Instead, the new product-bi-Kappa function shows more flexibility in modeling the gyrotropic VDFs with two distinct temperatures $T_{\parallel,\perp}$ and two distinct power indices $\kappa_{\parallel,\perp}$. A simple comparison of the contours plots show indeed a significant excess of anisotropy of the product-bi-Kappa by comparison to both the bi-Kappa and bi-Maxwellian models.

A further comparison with the contours plots of the measured distributions indicates two important results of our analysis. First, the bi-Kappa model is appropriate to describe particle distributions in the quiet and slow solar wind with a minimum strahl influence and, in general, small deformations of the halo. Secondly, the product-bi-Kappa (including the Maxwellian-Kappa) function seems to be adequate for modeling particle distributions in the fast solar wind with a prominent strahl component in the direction of magnetic field. Moreover, a double-strahl distribution looking just like the product-bi-Kappa contours can be observed near the magnetic large scale loops with electrons counterstreaming from both foot points.

The selfgenerated wave spectra originating from the Kappa models exhibit different properties. Thus, the wave instabilities constrains calculated for a bi-Kappa model do not fit with the halo limits in a slow solar wind as was expected, but those resulting from a product-bi-Kappa model seem to shape the halo electrons for any slow or fast solar wind. This suggests that the new product-bi-Kappa model incorporates in a proper way the excess of free energy expected to exist in anisotropic suprathermal plasmas. Assuming that the same wave fluctuations are the most plausible mechanism of acceleration and formation of suprathermal populations, we conclude pointing out the relevance of our study by the fact that an appropriate Kappa model enables a powerful selfconsistent analysis as it should be itself a product of particle acceleration by the selfexcited fluctuations.

Acknowledgements The authors acknowledge financial support from the Research Foundation Flanders (project G.0729.11), the KU Leuven (project GOA/2009-009, grant F/07/061), ESA Prodex 10 (project C 90205) and by the Deutsche Forschungsgemeinschaft (DFG), grant Schl 201/21-1. Financial support by the European Commission through the SOLAIRE Network (MTRN-CT-2006-035484), and the Seventh Framework Program (FP7/2007-2013) the grant agreement SWIFF (project nr. 2633430, www.swiff.eu) is gratefully acknowledged.

References

1. Marsch E. (2006). Kinetic physics of the solar corona and solar wind, *Living Rev. Solar Phys.* 3
2. Pierrard V. & Lazar M. (2010). Kappa distributions: theory and applications in space plasmas, *Sol. Phys.* 267, 153.
3. Hasegawa A., Mima K. & Duong-van N. (1985). Plasma distribution function in a superthermal radiation field, *Phys. Rev. Lett.* 54, 2608.
4. Miller J.A. & Roberts D.A. (1995). Stochastic proton acceleration by cascading Alfvén waves in impulsive solar flares, *Astrophys. J.* 452, 912.

5. Ma C. & Summers D. (1999). Correction to "Formation of Power-law Energy Spectra in Space Plasmas by Stochastic Acceleration due to Whistler-Mode Waves", *Geophys. Res. Lett.* 26, 1121.
6. Leubner M.P. (2000). Wave induced suprathermal tail generation of electron velocity space distributions, *Planet. Space Sci.* 48, 133.
7. Yoon P.H., T. Rhee & C.-M. Ryu (2006). Self-consistent formation of electron κ distribution: 1. Theory, *J. Geophys. Res.* 111, A09106.
8. Jokipii J.R. & M.A. Lee (2010). Compression acceleration in astrophysical plasmas and the production of $f(v) \sim v^{-5}$ spectra in the heliosphere, *Astrophys. J.* 713, 475.
9. Lin R.P. (1998). Wind observations of suprathermal electrons in interplanetary medium, *Space Sci. Rev.* 86, 61.
10. Fisk L.A. & Gloeckler, G. (2006). The common spectrum for accelerated ions in the quiet-time solar wind, *Astrophys. J.* 640, L79.
11. Schlickeiser R. (2002). *Cosmic Ray Astrophysics*, Springer, Heidelberg.
12. Pierrard V., Maksimovic M. & Lemaire J.F. (1999). Electron velocity distribution functions from the solar wind to corona, *J. Geophys. Res.* 104, 17021.
13. Hellinger, P.; Travnicek, P.; Kasper, J. C. & A. J. Lazarus (2006). Solar wind proton temperature anisotropy: Linear theory and WIND/SWE observations, *Geophys. Res. Lett.*, 33, L09101.
14. Stverak, S.; Travnicek, P.; Maksimovic, M. et al. (2008). Electron temperature anisotropy constraints in the solar wind, *J. Geophys. Res.*, 113, A03103.
15. Leubner M.P. (2002). A nonextensive entropy approach to kappa-distributions, *Astrophys. Space Sci.* 282, 573.
16. Summers D. & R.M. Thorne, 1991. The modified plasma dispersion function, *Phys. Fluids B* 3, 1835.
17. Hellberg M.A., R.L. Mace & T. Cattaert, 2005. Effects of superthermal particles on waves in magnetized space plasmas, *Space Sci. Rev.* 121, 127.
18. Lazar M., Schlickeiser R., Poedts S. & Tautz R. (2008). Counterstreaming magnetized plasmas with kappa distributions - I. Parallel wave propagation, *Mon. Not. R. Astron. Soc.*, 390, 168.
19. Lazar. M. & Poedts (2009). Firehose instability in space plasmas with bi-kappa distributions, *Astron. Astrophys.*, 494, 311.
20. Lazar. M., Schlickeiser, R., & Podts S. (2010). Is the Weibel instability enhanced by the suprathermal populations or not?, *Phys. Plasmas*, 17, 062112.
21. Lazar. M., Poedts, S. & Schlickeiser, R. (2011a). Instability of the parallel electromagnetic modes in Kappa distributed plasmas - I. Electron whistler-cyclotron modes, *Mon. Not. R. Astron. Soc.*, 410, 663.
22. Lazar. M., Poedts, S. & Schlickeiser, R. (2011b). Proton firehose instability in bi-Kappa distributed plasmas, *Astron. Astrophys.*, 534, A116.
23. Basu B. (2009). Hydromagnetic waves and instabilities in kappa distribution plasma, *Phys. Plasmas* 16, 052106.
24. Kasper, J. C.; Lazarus, A. J. & Gary S. P. (2002). Wind/SWE observations of firehose constraint on solar wind proton temperature anisotropy, *Geophys. Res. Lett.*, 29, 1839.
25. Bale S.D., Kasper J.C, Howes G.G. et al. (2009). Magnetic fluctuation power near proton temperature anisotropy instability thresholds in the solar wind, *Phys. Rev. Lett.* 103, 211101.
26. Pierrard V., Maksimovic M. & Lemaire J.F. (2001). Self-consistent model of solar wind electrons, *J. Geophys. Res.* 106, 29,305.
27. Pilipp W.G., Miggenrieder H., Montgomery M.D., et al. (1987a). Variations of electron distribution functions in the solar wind, *J. Geophys. Res.* 92, 1103;
28. Pilipp W.G., Miggenrieder H., Montgomery M.D., et al. (1987b). Unusual electron distribution functions in the solar wind derived from the Helios plasma experiment: double-strahl distributions and distributions with an extremely anisotropic core, *J. Geophys. Res.* 92, 1093;
29. Maksimovic M., Zouganelis I., J.-Y. Chaufray, et al. (2005). Radial evolution of the electron distribution functions in the fast solar wind between 0.3 and 1.5 AU, *J. Geophys. Res.* 110, A09104.

30. Cattaert, T., Hellberg, M.A., Mace, R.L. (2007). Oblique propagation of electromagnetic waves in a kappa-Maxwellian plasma, *Phys. Plasmas* 14, 082111.